Flow Fields Inside Stocked Fish Cages and the Near Environment

Lars C. Gansel
Norwegian University of Science and Technology,
Trondheim 7010, Norway
e-mail: Lars.Gansel@sintef.no

Siri Rackebrandt
Carl v. Ossietzky University Oldenburg,
Oldenburg 26129, Germany
e-mail: Siri.Rackebrandt@uni-oldenburg.de

Frode Oppedal
Institute of Marine Research,
Matredal 5984, Norway
e-mail: FrodeO@imr.no

Thomas A. McClimans
SINTEF Fisheries and Aquaculture,
Trondheim 7010, Norway
e-mail: Thomas.A.McClimans@sintef.no

This study explores the average flow field inside and around stocked Atlantic salmon (Salmo salar L.) fish cages. Laboratory tests and field measurements were conducted to study flow patterns around and through fish cages and the effect of fish on the water flow. Currents were measured around an empty and a stocked fish cage in a fjord to verify the results obtained from laboratory tests without fish and to study the effects of fish swimming in the cage. Fluorescein, a nontoxic, fluorescent dye, was released inside a stocked fish cage for visualization of three-dimensional flow patterns inside the cage. Atlantic salmon tend to form a torus shaped school and swim in a circular path, following the net during the daytime. Current measurements around an empty and a stocked fish cage show a strong influence of fish swimming in this circular pattern: while most of the oncoming water mass passes through the empty cage, significantly more water is pushed around the stocked fish cage. Dye experiments show that surface water inside stocked fish cages converges toward the center, where it sinks and spreads out of the cage at the depth of maximum biomass. In order to achieve a circular motion, fish must accelerate toward the center of the cage. This inward-directed force must be balanced by an outward force that pushes the water out of the cage, resulting in a low pressure area in the center of the rotational motion of the fish. Thus, water is pulled from above and below the fish swimming depth. Laboratory tests with empty cages agree well with field measurements around empty fish cages, and give a good starting point for further laboratory tests including the effect of fish-induced currents inside the cage to document the details of the flow patterns inside and adjacent to stocked fish cages. The results of such experiments can be used as benchmarks for numerical models to simulate the water flow in and around net pens, and model the oxygen supply and the spreading of wastes in the near wake of stocked fish farms. [DOI: 10.1115/1.4027746]

Introduction

The ventilation of cages used for aquaculture production is due to the water flow supplying oxygen and removing wastes. This basic relationship is essential for an effective production and ensuring animal welfare. Despite this fact, scarce information exists on the flow through cages holding biomasses of more than 1000 tons. The flow may be attenuated and redirected by a system of multiple cages, the netting of individual cages, the net fouling, and the biomass of the fish and their movement.

Based on trials with net panels, an increased drag force and attenuated flow is correlated with increased solidity (e.g., Refs. [1–4]). More comprehensive studies on single porous cylinders not only support stronger blockage of water with increased solidity but also display more qualitative information through streamlines ([5–8]). At low solidities, typical for clean nets, a uniform current allows large amounts of water to flow through the netting and create distinct local vortex streets in the wakes of the strands. At moderate solidities the vortex streets interact and create an additional blockage that forces more of the water around the porous cylinders. At high solidities the flow pattern is fairly similar to solid cylinders, but with recirculation pockets within as well as in the wake of the porous cylinder [7]. Solidity generally increases with fouling, which in turn varies over time and depth of the cage [9]. The net deformation increases with water speed while relative drag decreases ([10,11]) as more of the water flow is forced around the net cage, but the cage volume is reduced.

High biomasses of fish in cages will influence water flows in several ways. First, the biomass itself may act like a sponge, attenuating the current and redirecting it around the fish mass as noted by [12]. Second, the swimming behavior may generate vertical and/or horizontal currents as indicated by Refs. [13] and [14] in small-scale studies. These effects, however, are believed to fluctuate with the changing behavior of the fish. Typically, salmon are unevenly dispersed throughout the water column and congregate at certain depths in densities from 1.5 to 10 times the stocking density, depending on environmental conditions and internal motivational factors [15]. Variable vertical distributions of biomasses and fish densities will have depth-related flow impacts. Additionally, the schooling pattern of the fish and variable swimming speeds are thought to affect the flow differently. Salmon are known to swim along the net wall, producing a continuous school with a torus shape at the depth of peak biomass with variable vertical extension ([15,16]). Swimming speeds are normally registered as Body Lengths per second (BL/s) with a typical range of 0.2–1.9 BL/s during the illuminated day and less than 0.4 BL/s during the dark night ([15,16]). Low illumination may also lead to salmon spreading more evenly throughout the cage in the horizontal plane. The variable behavior and swimming speeds described will have diverse impacts on the water flow and must be taken into account to reach a comprehensive understanding of the ventilation of a fish cage.

This study aims at describing some of the basic influences of salmon and their movements on the water flowing through fish cages.

Material and Methods

Dye Experiments. Dye experiments were conducted at an experimental fish farm of the Institute of Marine Research in Matredal to the north of Bergen, Norway (see Fig. 1). A nontoxic, fluorescent dye (Fluorescein) was deployed in stripes across a

Contributed by the Ocean, Offshore, and Arctic Engineering Division of ASME for publication in the Journal of Offshore Mechanics and Arctic Engineering. Manuscript received July 7, 2011; final manuscript received May 20, 2014; published online June 12, 2014. Assoc. Editor: Hideyuki Suzuki.

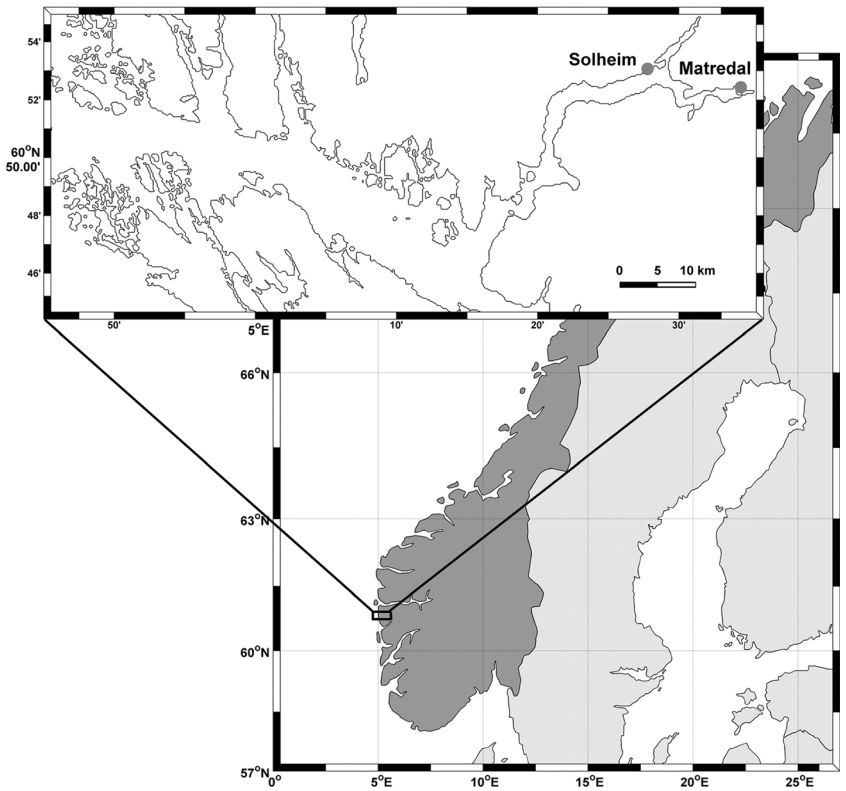

Fig. 1 Location of field experiments

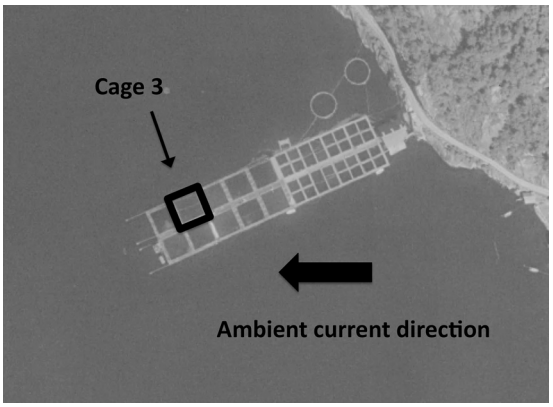

Fig. 2 Setup of the experimental fish farm of the Institute of Marine Research in Matredal, north of Bergen, Norway. Dye experiments were conducted in cage 3.

stocked fish cage to monitor the details of the surface currents in the cage.

Figure 2 shows the setup of the fish farm and the location of the test cage (cage 3). An aqueous solution of the dye was pumped through two tubes, which were pulled over the cage about 30 cm above the surface. A Sony Handycam (HDR-CX 505VE) was mounted at about 25 m height to 5 weather balloons filled with helium. The camera faced down and continuously recorded the deployment and spreading of the dye. Cage 3 was 12 m long, 12 m wide, and 12 m deep and the stocking density was 19 kg/m^3. The adjacent cages were empty and there was no feeding activity during the experiments. The netting in cage 3 was clean with a porosity (the percentage of the area of openings of the overall net area) of approximately 80%. The ambient current was from the east (Fig. 2) and the wind velocity was very small during the experiments. Flow patterns on the surface were obtained by tracking single, dense blobs of dye. The flow velocity outside of the fish cage was estimated from the spreading velocity of dye deployed outside of the cage.

The experiment was repeated three times within one hour and two examples are illustrated in Figs. 3 (31.10.2009, 14:57) and 4 (31.10.2009, 15:10) in the Results section.

Current Measurements. The flow was measured around a single fish cage at the Solheim site of the Institute of Marine Research (Fig. 1). The location of the fish cage in the array of fish cages is shown in Fig. 5.

A round cage with a diameter of 12 m and a depth of 12 m was installed at location 5 (Fig. 5, left). Cages 3, 4, 6, 7, and 8 were empty and without nettings during the measurements. Currents were measured with NORTEK vector current meters at 5 locations (Fig. 5, right) around cage 5 during two periods: period 1 (Aug. 22 and 23, 2008, 25 h continuous measurements) with no fish present and period 2 (Sept. 2–4, 2008, 50 h continuous measurements) with the cage stocked with 7663 salmon (*Salmo salar* L.) of a total biomass of about 12 t equivalent to 8.8 kg/m^3. The fish farm at Solheim was constructed with a rigid frame (similar to the frames seen in Fig. 2) and the locations of the current meters were measured with tape measures in relation to the metal frame of the fish farm. The depth of the vector instruments was cycled so that one depth profile of the current direction and speed was obtained each hour during both measurement periods. The instruments remained at each depth for at least 5 min to ensure a sufficient amount of data for time averaging. A NORTEK Aquadopp current profiler was mounted about 60 m to the north east of cage 5 (Fig. 5(*a*)). The current profiler continuously recorded the current speed and direction between depths of 2.5 m and 30.5 m with a depth resolution of 2 m and a temporal resolution of 10 min. At the Solheim site, an echo-sounder ([17,18]) was mounted below cage 5 to monitor vertical distribution of the fish. The observed fish density (OFD) in kg/m^{-3} in each depth interval ($_n$) was calculated as $\mathrm{OFD}_n = B\ \mathrm{ER}_n\ \mathrm{V}_n^{-1}$, where B is total biomass in the cage,

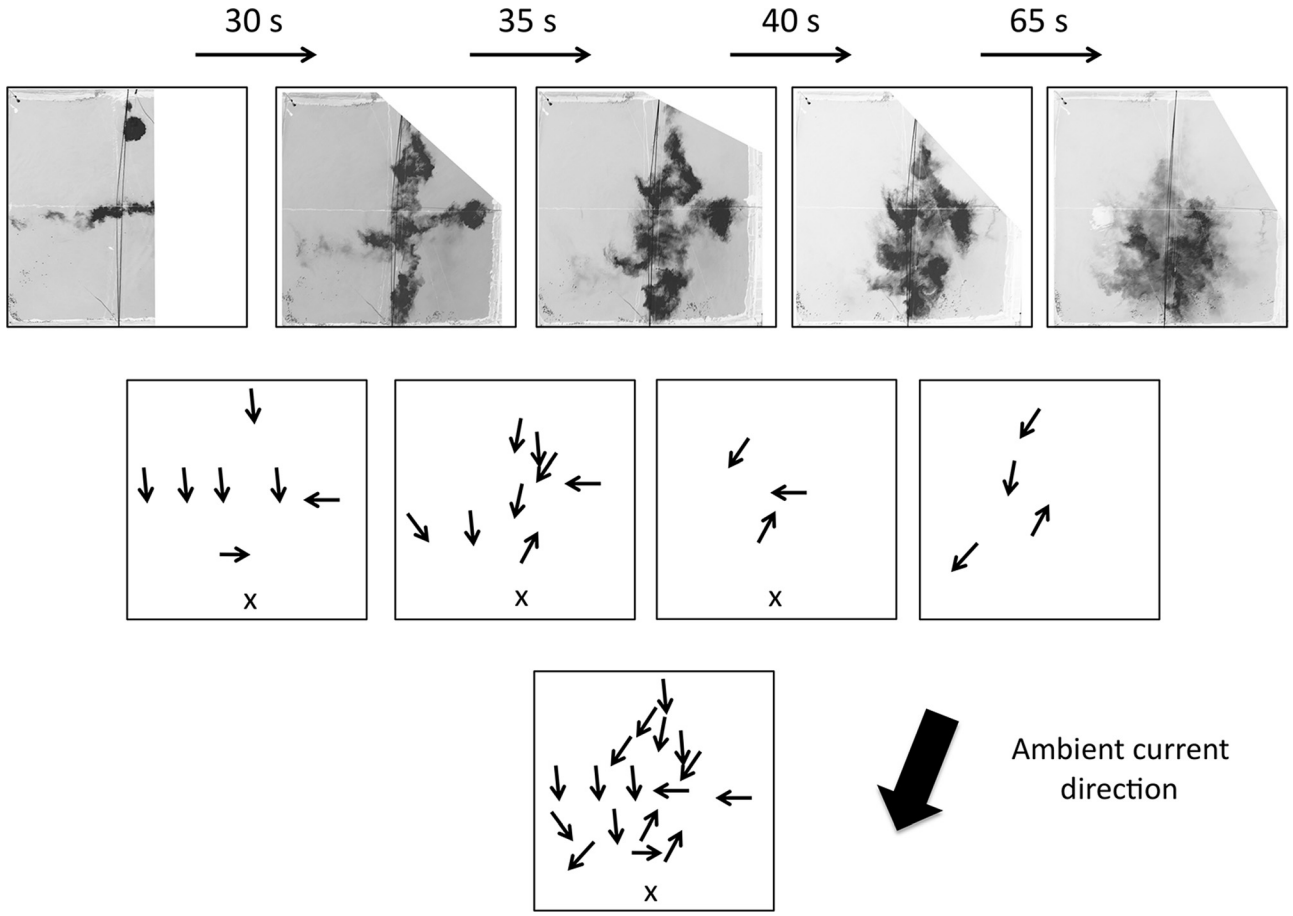

Fig. 3 Dye spreading in cage 3 within the first 170 s at 14:57 (Oct. 31, 2009). The arrows indicate the flow direction and are obtained by tracking the movement of dye blobs between two pictures. The lowest plot is a combination of the arrow plots in the middle. The ambient flow speed was approximately 0.06 m/s.

ER is the relative echo intensity, and V is the volume of the 0.5 m depth interval (72 m^3). A camera with an IR light source was mounted inside cage 5 to determine the swimming speed of fish in BL/s by noting the time it takes one fish to pass a fixed point in the fish cage. The average swimming speed of 20 individual, randomly chosen fish was determined at three different depths (3 m, 7 m, and 10 m) every hour. An overview of the instrumentation during periods 1 and 2 is given in Table 1. To assess the importance of density stratification at the facility, conductivity, temperature, and depth (CTD) profiles were measured.

Any blockage effect by the netting of cage 5 and the effect of fish inside the cage can be observed as a deflection of the ambient current and by a change in current speed at different locations around the cage. The count of 5 current meters around the fish cage ensured that there would be at least one current meter in each quadrant. If the netting or the fish lead to a blockage, the deflection of the ambient current in the upstream quadrants should be away from the center of the fish cage. It is therefore important to know the upstream ambient current. The setup of the experiments allowed the deduction of the ambient current just upstream from cage 5 from two different data sources: the current profiler and the vector instruments in the upstream quadrants. Each of these data sources alone could lead to poor estimates of the current direction upstream from cage 5. The current profiler recorded all the relevant information on the current at its location, but the location of the fish farm close to the shore in a fjord made a second measure of the current direction necessary as a control. With simultaneous current measurements from many current meters around a fish cage, the ambient current direction and speed could be determined as the average of the values attained from all current meters. The average current direction from all 5 vector instruments integrated over the first 15 m depth agreed well with the current direction measured by the current profiler (see Table 2). The average current direction used in the Results section is the average of the direction of all 5 vector instruments at the given time and depth. Thus, the results in Table 2 determine the upstream and downstream quadrants.

The vector current meters measured the velocity with a frequency of 1 Hz. All flow data originating from vector instruments presented in this article are time averages of 240 s (i.e., 240 samples).

Results

Dye Experiments. Figures 3 and 4 show the spreading of dye within the same stocked fish cage (12 m × 12 m) at different times. The stocking density was about 19 kg/m^3 and the fish were swimming in circles along the netting of the cage. The dye converges toward a point that is offset downstream from the center of the fish cage. The offset is about 1/6 of the length of the cage with an ambient current speed of 0.06 m/s (Fig. 3) and about 2/6 of the length of the cage with an ambient current speed of 0.09 m/s (Fig. 4). Figure 3 shows a flow opposite to the ambient current direction south from the center of the cage. The flow direction is to the south or south east to the west and south west from the center and to the south or south west, north from the center of the fish cage. East from the center, the flow direction is to the west. The combination of these dye spreading patterns yields a rotational flow field. Figure 4 shows a similar general pattern during a period

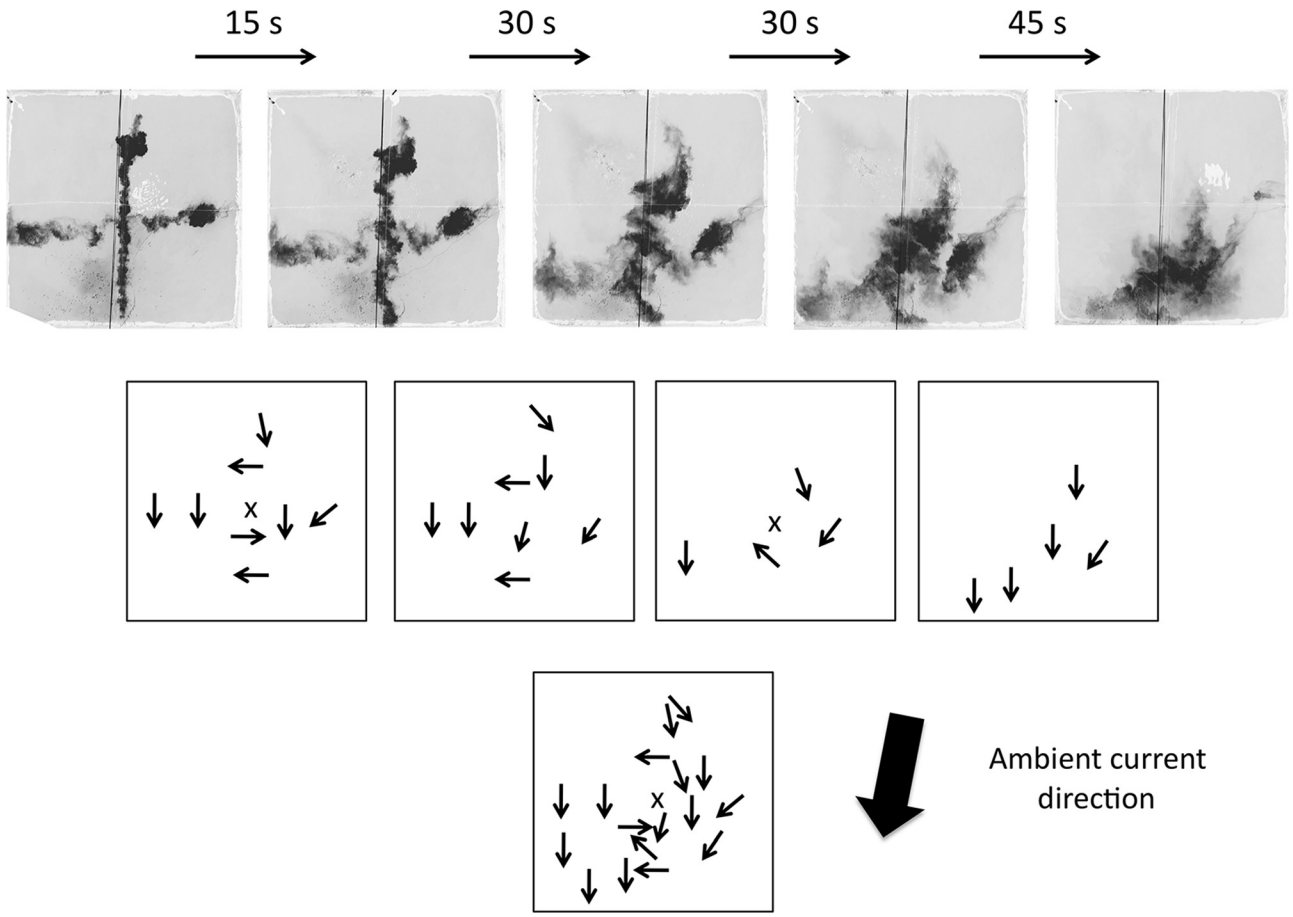

Fig. 4 Dye spreading in cage 3 within 120 s at 15:10 (Oct. 31, 2009). See Fig. 4 for details. The ambient flow speed was approximately 0.09 m/s.

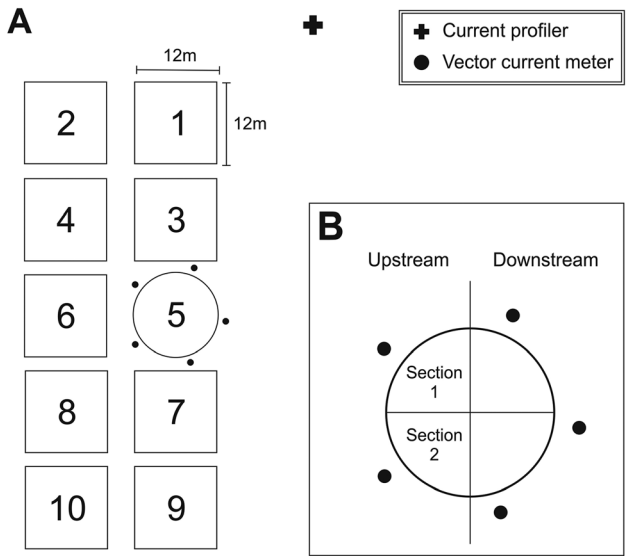

Fig. 5 Setup of the current measurements at the Solheim site. 3A shows the location of cage 5 in the fish farm setup and 3B shows cage 5 only. The dots mark the positions of 5 NORTEK vector current meters.

with a higher ambient current speed, but the flow directions seem to be deflected toward the direction of the ambient current. The flow direction south from the center of the cage is perpendicular to the direction of the ambient flow. The dye spreads to the south west and south west from the center of the cage.

Table 1 Overview of the measurements during measurement periods 1 and 2

Period	Date	Stocking density (kg/m^3)	Instruments
1	Aug. 22 and 23, 2008	No fish	Vector Profiler CTD
2	Sept. 2–4, 2008	8.8	Vector Echosounder
			Camera Profiler CTD

Table 2 Compass direction of the ambient current as recorded by the current profiler within the first 15 m depth and as the average from the directions recorded by 5 vector instruments within the first 15 m depth around cage 5

Date/Time	Direction from profiler (deg)	Direction from vectors (deg)
Aug. 22, 2008, 17:00	238	238
Aug. 23, 2008, 07:00	241	243
Sept. 2, 2008, 17:00	238	229
Sept. 2, 2008, 23:00	46	63
Sept. 4, 2008, 12:00	38	48

Figures 3 and 4 show convergence of surface water toward a location with an offset from the center of the cage in the ambient current direction. Surface water is not flowing toward this point on straight paths, but has vorticity and moves in a circular pattern (called swirl).

Stratification. Representative density profiles for the two sets of experiments at the Solheim site are shown in Fig. 6. The upper

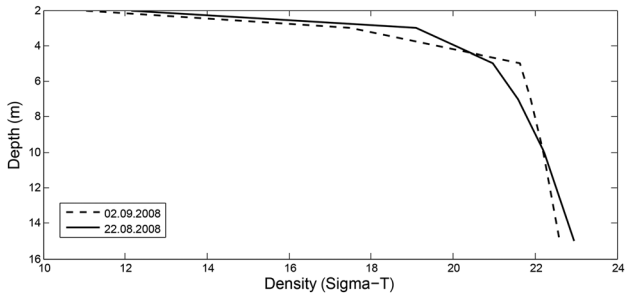

Fig. 6 Variation of density with depth at Solheim on Aug. 22, 2008 and on Sept. 2, 2008. (Sigma-T is density minus 1000 kg/m^3.)

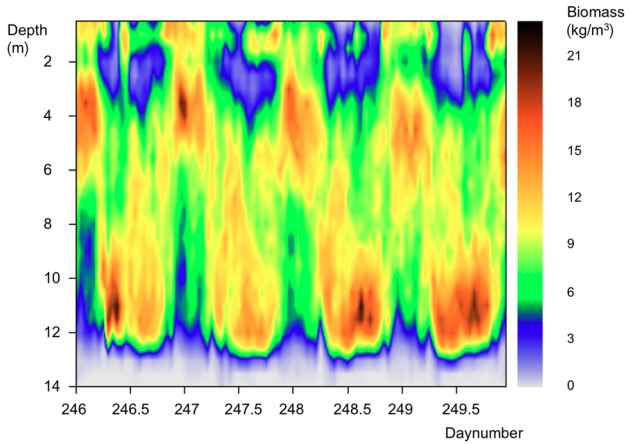

Fig. 7 Vertical distribution of fish biomass from Sept. 2, 2008 to Sept. 5, 2008. Full day numbers mark midnight.

4 m reveal a typical fjord halocline, while there was a slow increase in density with depth below 6 m. The characteristic wave speed of internal disturbances at the pycnocline is of order 0.5 m/s, so the flows in this region are highly sub-critical (densimetric Froude numbers much smaller than 1).

Biomass Distribution. Figure 7 shows a strong diurnal variation of the vertical distribution of fish biomass between Sept. 2, 2008 and Sept. 5, 2008. At night, most fish were between 2 m and 6 m depth at densities of up to 22 kg/m^3. During daytime, the highest fish densities of up to 23 kg/m^3 were between 10 m and 12 m depth. The stocking density in this fish cage was 8.8 kg/m^3.

Current Measurements. Figures 8 and 9 show the direction and speed of the currents measured by the 5 vector instruments around cage 5 without fish (see Fig. 5 for the setup). On Aug. 22, 2008 at 17:00 (Fig. 8), the current direction recorded by the vector instruments show only minor deviations from the ambient flow direction at 2 m, 8 m, and 15 m depth. Deviations >10 deg occur only at 4 m depth. However, both vector instruments on the upstream half of the fish cage registered a deflection of the ambient current in the same direction.

On Aug. 23, 2008 at 07:00 (Fig. 9), large deviations from the ambient current direction at the location of the vector instruments occurred at depths of 2 m and 8 m, but not at 4 m and 15 m depth. The deviations of the current direction on the upstream half of cage 5 were in the same direction at 2 m depth (Fig. 9(*a*)), while they were directed away from the center of the cage at 8 m depth (Fig. 9(*c*)).

Figures 10–12 show the currents around cage 5 stocked with about 12 t of fish. Large deviations ($\gg$ 10 deg) of direction from the ambient current away from the center of the cage in the front

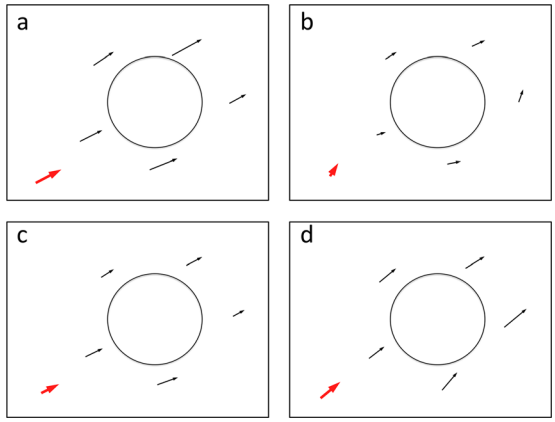

Fig. 8 Current direction and speed at five locations around cage 5 (see Fig. 3) at four different depths on Aug. 22, 2008 at 17:00. Figures (*a*)–(*d*) show the currents at 2 m, 4 m, 8 m, and 15 m, respectively. The length of the arrows indicates the current speed and the orientation of the arrows indicates the current direction. The black arrows are the results from the 5 current meters. The bold arrow in the lower left corner shows the ambient current.

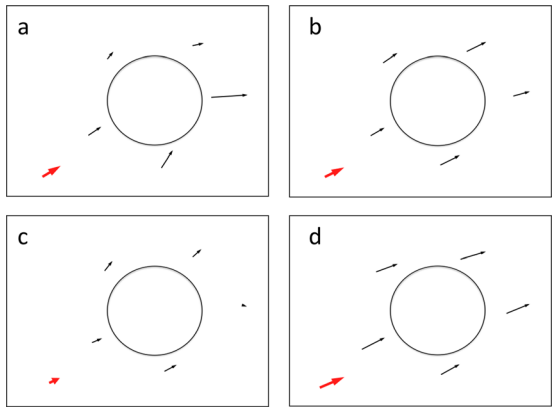

Fig. 9 Same as Fig. 8, but for Aug. 23, 2008 at 07:00

quarters occurred at 10 m depth on Sept. 2, 2008 at 17:00 (Fig. 10(*d*)), at 10 m and 12 m depth on Sept. 4, 2008 at 12:00 (Figs. 11(*c*) and 11(*d*)) and at 4 m depth on Sept. 2, 2008 at 23:00 (Fig. 12(*b*)). There are large deviations of the ambient current at 2 m depth in all of the above cases, but the deviations do not follow a common pattern.

Table 3 shows differences in the current speed upstream ($V_{\text{upstr.}}$) and downstream ($V_{\text{downstr.}}$) of cage 5. On Aug. 22, 2008 and Aug. 23, 2008 the fish cage was empty. Measurements on these dates showed some variability in V_r (the ratio between $V_{\text{upstr.}}$ and $V_{\text{downstr.}}$) with depth, but there is no consistent common pattern. On Sept. 2, 2008 at 17:00 and Sept. 4, 2008 at 12:00, a high fish biomass was at depths of 5 m–12 m (Fig. 7). At these times, the depth of high fish density coincided with relatively low current speeds and a $V_r \gg 1$, while $V_r < 1$ at depths with low fish biomass. No clear pattern of the variability of V_r with depth occurred on Sept. 2, 2008 at 23:00, when there was a high fish density at 4 m depth.

For a display of the current speed in Table 3, the 5 vector instruments around cage 5 were divided into instruments on the upstream side and the downstream side of the fish cage. This division is dynamic and dependent on the ambient flow direction. The fish cage is separated through its center by a line normal to the ambient current direction (Table 2). Vector instruments on the upstream half are located in the upstream quadrants, that is toward the incoming ambient current and instruments on the downstream half are located downstream from the dividing line.

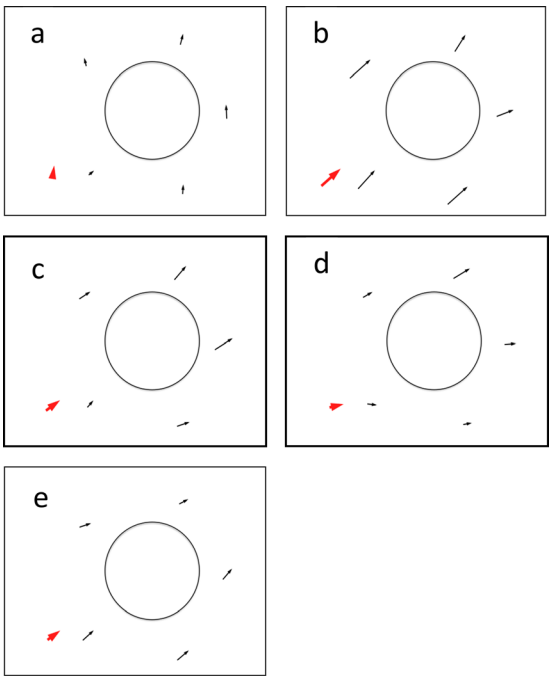

Fig. 10 Same as Fig. 8, but *d* is for 10 m depth and *e* is for 12 m depth and for Sept. 2, 2008 at 17:00

The swimming speed of fish in cage 5 was lowest close to the surface (Table 4). The swimming speed was about 0.8 BL/s on Sept. 2, 2008 at 17:00 and Sept. 4, 2008 at 12:00 at depths with high fish densities (10 m and 11 m, respectively). Fish were swimming in circles along the net of the cage. On Sept. 2, 2008 at 23:00, the highest biomass was close to the surface and here fish were holding position in the current.

Discussion

Dye spreading experiments with a stocked fish cage showed a convergence of surface water toward a central location with an offset from the center of the fish cage in the ambient current direction. This offset was larger when the ambient current speed at the surface was faster. The porosity of the netting was about 80%. Reference [6] showed an almost constant flow direction inside empty cages with a similar porosity in a uniform flow. Variability in the ambient flow alone can not explain the convergence of surface water. Furthermore, the flow was found to rotate. This observation agrees with the findings of Ref. [13], who reported a rotational pattern in the surface water flow inside stocked fish cages. Recently, Ref. [19] observed a rotation of the water flow within a large commercial fish cage. A convergence of water at the surface has to be associated with a downwards-directed vertical flow and a spin-up of the ambient surface vorticity.

Reference [14] reported that water exited a fish cage in all directions at the depth of maximum fish biomass during small scale experiments with stocked fish cages with a volume of 1 m^3. This observation fits well with the findings of Ref. [17], who reported a downwards-directed flow in the center of the cage within a commercial salmon cage at depths of high fish density swimming in a torus-shaped volume. Fish swimming in circles get their centripetal force to accelerate toward the center by pushing water away from the center. This creates a low pressure in the center of the cage and draws water from above and below. Reference [20] observed a downwards-directed flow upstream from a fish cage and an upwards-directed flow downstream from the cage at the depth of highest fish density.

During the dye experiments presented in this study, the main biomass of the fish was in the pycnocline between 2 m and 5 m depth and the fish were circling in the cage. The stratification limits the vertical extent of the fish-induced circulation. The above scenario should therefore apply and is very likely due to the following reasons: a suction of surface water would lead to convergence and rotation, which would lead to the formation of a swirl in the center of the fish cage. The swirl depends on the background vorticity in the converging surface flow. This depends on the ambient vorticity and that induced by the fish. The offset of the center of the swirl, as seen from the present data (Figs. 3 and 4), is most likely caused by the ambient current penetrating into the fish cage, thereby deflecting the flow inside the cage in the ambient current direction.

Dye tracking proved to be very useful for the investigation of surface flow patterns inside fish cages by following small water volumes with high dye concentrations. The use of dye tracking in field experiments based on aerial videos or images is restricted to the estimation of horizontal flow velocities close to the surface, but it can give qualitative as well as quantitative data (if reference distances are available on videos/images). The use of fluorescent dye allows concentration measurements with fluorometers. However, in this study the authors were mostly interested in qualitative data (flow patterns).

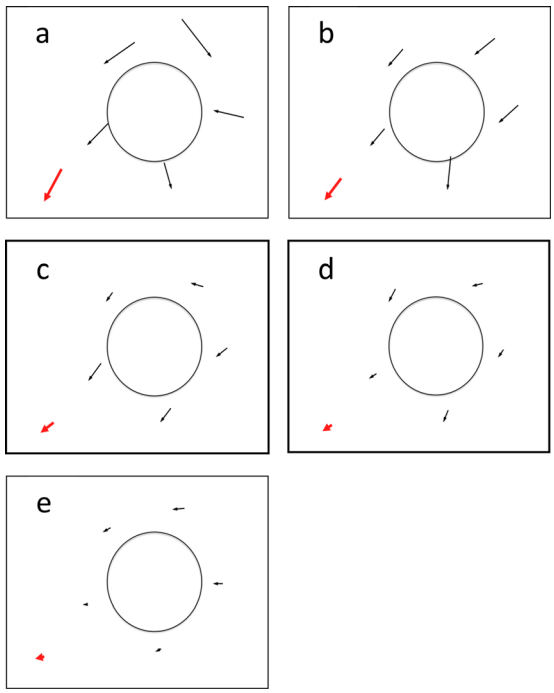

Fig. 11 Same as Fig. 10, but for Sept. 4, 2008 at 12:00

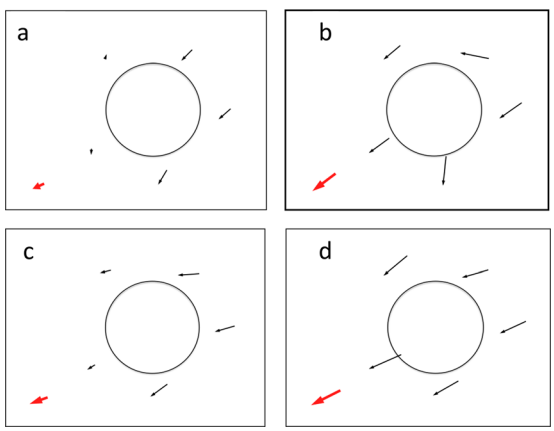

Fig. 12 Same as Fig. 8, but for Sept. 2, 2008 at 23:00

Table 3 Distribution of the average horizontal flow speed over the upstream and downstream half of the fish cage at 5 different times. $V_{upstr.}$ and $V_{downstr.}$ are the average speed over the upstream half and downstream half of the fish cage, respectively. The fish cage was empty on Aug. 22, 2008 and Aug. 23, 2008 and stocked from Sept. 2, 2008 onwards. White marks the measurements around the empty cage and gray marks the depth with the highest fish biomass during the indicated measurement times.

Date/Time	Depth (m)	$V_{upstr.}$ (m/s)	$V_{downstr}$ (m/s)	V_r ($V_{downstr.}$ /$V_{upstr.}$)
Aug. 22, 2008, 17:00	2	0.057	0.057	1.00
Aug. 22, 2008, 17:00	4	0.024	0.028	1.16
Aug. 22, 2008, 17:00	8	0.039	0.032	0.81
Aug. 22, 2008, 17:00	15	0.046	0.055	1.22
Aug. 23, 2008, 07:00	2	0.039	0.040	1.04
Aug. 23, 2008, 07:00	4	0.044	0.035	0.79
Aug. 23, 2008, 07:00	8	0.0200	0.023	1.18
Aug. 23, 2008, 07:00	15	0.052	0.053	1.01
Sept. 2, 2008, 17:00	2	0.019	0.017	0.94
Sept. 2, 2008, 17:00	4	0.056	0.039	0.70
Sept. 2, 2008, 17:00	10	0.023	0.040	1.75
Sept. 2, 2008, 17:00	12	0.018	0.031	1.70
Sept. 2, 2008, 17:00	15	0.028	0.024	0.84
Sept. 2, 2008, 23:00	2	0.024	0.023	0.93
Sept. 2, 2008, 23:00	4	0.056	0.058	1.04
Sept. 2, 2008, 23:00	10	0.038	0.031	0.83
Sept. 2, 2008, 23:00	15	0.062	0.070	1.13
Sept. 4, 2008, 12:00	2	0.086	0.067	0.78
Sept. 4, 2008, 12:00	4	0.056	0.054	98
Sept. 4, 2008, 12:00	10	0.028	0.034	1.22
Sept. 4, 2008, 12:00	12	0.0200	0.024	1.22
Sept. 4, 2008, 12:00	15	0.0220	0.011	0.51

During flow measurements around an empty fish cage on Aug. 22, 2008 and Aug. 23, 2008, large deviations from the ambient current on the upstream side of the cage were found only at depths of 4 m on Aug. 22, 2008 (Fig. 8) and at depths of 4 m and 8 m on Aug. 23, 2008. The interaction of the cage and the stratified flow may have caused internal waves at these depths. A blockage of the ambient current by the fish cage should lead to a deviation of the ambient current away from the center of the cage in the upstream quarters. At 4 m depth, the currents in these sections were deflected in the same direction on both dates. The deflection away from the center of the cage at 8 m depth on Aug. 23, 2008 might suggest a blockage of the ambient current by the fish cage. However, a large deviation occurred only on one side of the cage. Furthermore, if the fish cage were to block the flow, the blockage should lead to a deflection of the ambient current direction at all depths down to 12 m. This is not the case, which leads to the conclusion that the empty fish cage did not cause a significant blockage and that the anomalies were due to internal wave disturbances.

Large (>10 deg) deviations from the ambient current direction around the stocked fish cage (Figs. 10–12 and Table 3) suggest that blockage occurred at depths with maximum fish biomasses but not at depths with low fish densities. On Sept. 4, 2008, the maximum biomass density was higher and the deflection of the ambient current at the maximum biomass depth was stronger than on Sept. 2, 2008 at 17:00 (see Figs. 7, 10, and 11). On Sept. 2, 2008 at 23:00 the maximum biomass density was even higher between 3 m and 4 m depth (Fig. 7). Fish at this depth did not swim in circles, but held their position in the current. Figure 12 shows a strong deflection of the ambient current around the fish cage at 4 m depth, which leads to the assumption that a high fish density (and probably an additional input of turbulence in the wake of the fish cage due to the motion of the fish to hold their location) is enough to cause a blockage to the ambient current. However, the deflection of the ambient current is almost as strong

Table 4 Swimming speed of the fish in cage 5 in body lengths per second (BL/s). The values given for swimming speed are calculated as the mean value of the swimming speeds of 20 individual fish.

Date/Time	Depth (m)	Swimming speed (BL/s)
Sept. 2, 2008, 17:00	4	0.6
	8	0.9
	11	0.8
Sept. 2, 2008, 23:00	3	0.0
	7	0.3
	10	0.5
Sept. 4, 2008, 12:00	3	0.6
	7	0.6
	10	0.8

on Sept. 2, 2008 at 17:00 at 12 m depth, where the fish biomass was lower than at 4 m depth on Sept. 2, 2008 at 23:00 but the fish were circling in the cage (see Figs. 7, 10, and 12). On Sept. 4, 2008 at 12:00, a maximum biomass density lower than on Sept. 2, 2008 at 23:00 and higher than at Sept. 2, 2008 17:00, combined with circling of the fish led to the strongest deflection of the ambient current (see Figs. 7, 10–12). Therefore, circular swimming motion of fish in the cage seems to cause an additional blockage to an ambient current.

A consistent pattern occurred in the ratio of the upstream and downstream flow speeds when fish were circling in the cage at high densities: at the depth with the highest fish density the flow speed downstream of the cage is much higher than in the upstream region. This pattern did not occur around the empty cage or on Sept. 2, 2008 at 23:00, when most fish were holding position in the current between 3 m and 4 m depth. Fish holding position create turbulence, but no net momentum transfer to the flow, as the drag force on the fish equals the thrust force created by the swimming motion. Fish swimming in circles or back and forth, on the other hand, create a force that pushes water outwards. Salmon are known to swim in a circular pattern along the nets of fish cages in high densities during the day [15,16]. Fish swimming in circles, pushing water outwards, create a water flow reducing the flow speed in the upstream half of the cage, but increasing the flow speed in the downstream half at their swimming depth.

The dye spreading experiments and the flow measurements outside of a fish cage were conducted at different times and locations and the form of the cages was different (square and circular). However, the size of the cages was similar in all tests and both cages used in the experiments were part of similar fish farms with the adjacent cages being empty. The focus of this study is on quantitative effects of fish biomass and swimming activity on the water flow past stocked cages and based on the above discussion of the experiments we assume the mentioned generalizations to be valid for comparable conditions (fish cage size, net solidity, biomass, swimming speed and flow speed). Thus, the outcomes from both studies can be combined to form a general model for the effect of fish inside net cages. The main findings are summarized as follows.

The fish biomass inside fish cages is often not distributed equally throughout the volume of the cages. Instead, high fish densities are found at certain depths. During the dark night, salmon swimming speeds may be very low [15,16] or just sufficient to hold position in the current. However, high fish densities seem to cause a deflection of the ambient current, forcing some water around the cage, even if the fish are not swimming in circles inside the cage. Both their volume and displacement thickness of their wakes in the region of adjustment cause a local disturbance to the ambient flow. Fish swimming in circles around the center of a net cage seem to lead to a stronger water blockage than fish standing in the current. The circular motion of a large biomass (the swimming fish) can lead to water being pushed out of the cage as a result of forces necessary to counter the acceleration of fish toward the center of the cage. Water pushed out by the fish is

replaced from the surface (Figs. 3 and 4) and probably also from depths below the depth of maximum fish density. The convergence in these layers is associated with a spin-up of ambient vorticity and the creation of swirl in the cage by the fish propulsion. In the present data (Figs. 3 and 4), the swirl was in the same direction as the fish motion. Unpublished observations from other cages suggested a swirl opposing the fish motion. In these studies, however, the environmental conditions were not measured. At very low ambient currents, this enhanced circulation improves the ventilation of the cage. Laboratory studies of fish-induced motions in uniform flows can reveal the role of fish-induced vorticity on the swirl of the converging flows.

The present experiments were performed in 12 m size cages, raising the question of scaling to large (up to 50 m) commercial cages. The fish swimming speeds and volumes are related to their size, but the acceleration needed to keep them in a circular path is inversely proportional to the distance from the center. Fish behavior suggests that the main school will be a torus in the outer portion leading to a broader central convergence zone and reduced lateral circulation. This is assuming that the stocking density is the same.

Conclusions

Salmon schools swimming in circles within a fish cage induce an outflow at school depth that blocks the incoming flow. The circulation of the fish-induced flow causes a recirculation at other depths, effectively increasing the volume of water that ventilates the cage. The present results show a consistent picture of the process, but to obtain high-quality benchmarks for the development of numerical models that can produce these flows and model the oxygen supply and the spreading of wastes in the near wake of stocked fish farms we recommend controlled laboratory simulations including controlled fish-induced circulations.

Acknowledgment

The work was performed through a Ph.D. Fellowship from the Faculty of Engineering Science and Technology at the Norwegian University of Science and Technology. The work was partly financed by the Norwegian Research Council through the projects *INTEGRATE* and *SECURE* and the center *CREATE* at SINTEF Fisheries and Aquaculture. The authors thank Dag Myrhaug for support and Steffen Maron, Simone Balzer, and Iwe Muiser for their help on the fish farms.

References

[1] Løland, G., 1991, "Current Force on and Flow Through Fish Farms," Ph.D. thesis, Division of Marine Hydrodynamics, The Norwegian Institute of Technology, Trondheim, Norway.

[2] Zhan, J. M., Jia, X. P., Li, Y. S., Sun, M. G., Guo, G. X., and Hu, Y. Z., 2006, "Analytical and Experimental Investigation of Drag on Nets of Fish Cages," Aquacultural Eng., **35**, pp. 91–101.

[3] Patursson, O., 2008, "Flow Through and Around Fish Farming Nets," Ph.D. thesis, Ocean Engineering, University of New Hampshire, Durham, NH.

[4] Patursson, Ø., Swift, R., Tsukrov, I., Simonsen, K., Baldwin, K., Fredriksson, D. W., and Celikkol, B., 2010, "Development of a Porous Media Model With Application to Flow Through and Around a Net Panel," Ocean Eng., **37**, pp. 314–324.

[5] Gansel, L. C., McClimans, T. A., and Myrhaug, D., 2012, "The Effects of Fish Cages on Ambient Currents," ASME J. Offshore Mech. Arctic Eng. **134**(1), p. 011303.

[6] Gansel, L. C., McClimans, T. A., and Myrhaug, D., 2012, "Flow Around the Free Bottom of Fish Cages in a Uniform Flow With and Without Fouling," J. Offshore Mech. Arctic Eng., **134**(1), p. 011501.

[7] Gansel, L. C., McClimans, T. A., and Myrhaug, D., 2010, "Average Flow Inside and Around Fish Cages With and Without Fouling in a Uniform Flow," 29th ASME International Conference on Offshore Mechanics and Arctic Engineering (OMAE 2010), Shanghai, China, June 6–11, Paper No. OMAE2010-20481.

[8] Harendza, A., Visscher, J., Gansel, L., and Pettersen, B., 2009, "PIV on Inclined Cylinder Shaped Fish Cages in a Current and the Resulting Flow Field," 27th ASME International Conference on Offshore Mechanics and Arctic Engineering (OMAE2008), Estoril, Portugal, June 15–20, Paper No. OMAE2008-57746.

[9] Guenther, J., Misimi, E., and Sunde, L. M., 2010, "The Development of Biofouling, Particularly the Hydroid Ectopleura Larynx, on Commercial Salmon Cage Nets in Mid-Norway," Aquaculture, **300**, pp. 120–127.

[10] Lader, P., Dempster, T., Fredheim, A., and Jensen, Ø., 2008, "Current Induced Net Deformations in Full-Scale Cages for Atlantic Salmon (Salmo Salar)," Aquaculture Eng., **38**, pp. 52–65.

[11] Moe, H., Fredheim, A., and Hopperstad, O. S., 2010, "Structural Analysis of Aquaculture Net Cages in Current," J. Fluids Struct., **26**, pp. 503–516.

[12] Johansson, D., Juell, J.-E., Oppedal, F., Stiansen, J.-E., and Ruohonen, K., 2007, "The Influence of the Pycnocline and Cage Resistance on Current Flow, Oxygen Flux and Swimming Behaviour of Atlantic Salmon (Salmo salar L.) in Production Cages," Aquaculture, **265**, pp. 271–287.

[13] Inoue, H., 1972, "On Water Exchange in a Net Cage Stocked With the Fish, Hamachi," Bull. Jpn. Soc. Sci. Fish., **38**, pp. 167–176 (in Japanese).

[14] Chacon-Torres, A., Ross, L. G., and Beveridge, M. C. M., 1988, "The Effects of Fish Behaviour on Dye Dispersion and Water Exchange in Small Net Cages," Aquaculture, **73**, pp. 283–293.

[15] Oppedal, F., Dempster, T., and Stien, L., 2011, "Environmental Drivers of Atlantic Salmon Behaviour in Sea-Cages: A Review," Aquaculture, **311**, pp. 3–18.

[16] Juell, J. E., 1995, "The Behavior of Atlantic Salmon in Relation to Efficient Cage-Rearing," Rev. Fish. Biol. Fisher., **5**, pp. 320–335.

[17] Bjordal, Å., Juell, J. E., Lindem, T., and Fernö, A., 1993, "Hydroacoustic Monitoring and Feeding Control in Cage Rearing of Atlantic Salmon (*Salmo salar* L.)," *Fish Farming Technology*, H. Reinertsen, L. A. Dahle, L. Jørgensen, and K. Tvinnereim, eds., Balkema, Rotterdam, pp. 203–208.

[18] Oppedal, F., Juell, J. E., and Johansson, D., 2007, "Thermo- and Photoregulatory Swimming Behaviour of Caged Atlantic Salmon: Implications for Photoperiod Management and Fish Welfare," Aquaculture, **265**, pp. 70–81.

[19] Nilsen, A., Bjøru, B., Vigen, J., Oppedal, F., and Høy, E., 2010, "Evaluering av Metoder for Badebehandling mot lakselus i Stormerd," Veterinærinstituttets rapportserie, 17-2010, Veterinærinstituttet, Oslo, Norwegian, p. 48.

[20] Rackebrandt, S., 2008, "Water Flow in and Around Fish Cages," Report to Marine Constructions, University of Science and Technology, Trondheim, Norway.